OPTIMIZING THE PERFORMANCE OF A HEAT ENGINE: A SIMULATION STUDY

By

Mehari Bayou Zerihun

SUBMITTED IN PARTIAL FULFILLMENT OF THE
REQUIREMENTS FOR THE DEGREE OF
MASTER OF SCIENCE IN PHYSICS
AT
ADDIS ABABA UNIVERSITY
ADDIS ABABA, ETHIOPIA
DECEMBER 2010

ADDIS ABABA UNIVERSITY

DEPARTMENT OF

PHYSICS

Supervisor: _____

Dr.MULUGETA BEKELE

Examiners: _____

Dr.TATEK YERGOU

_____

Dr.LEMI DEMEYU

ADDIS ABABA UNIVERSITY

Date: **December 2010**

Author: **Mehari Bayou Zerihun**

Title: **OPTIMIZING THE PERFORMANCE OF A HEAT ENGINE: A SIMULATION STUDY**

Department: **Physics**

Degree: **M.Sc.** Convocation: **December** Year: **2010**

Signature of Author

For my friends ...

Table of Contents

List of Figures

Acknowledgements

I would like to express my sincere gratitude to my advisor Dr.Mulugeta Bekele for his unreserved support, valuable advice and friendly approach. While working with him, I have got a chance to share his long research experience which benefitted me a lot. I would like also to thank Dr.Tatek Yergou for invaluable supports he provided me while working this thesis

I am extremely grateful to my lovely friends in Physics Department of statistical and computational group, who were graduates of 2010, for the constant support they provide to me. I would also like to thank my former Computational Physics teacher Yeneneh Yalew.

It gives me a great pleasure to acknowledge the Department of Physics and the School of Graduate studies, Addis Ababa University for the support I get during my study.

Abstract

We performed a simulation study of a simple heat engine as it undergoes Carnot-type cyclic motion in a finite time over a wide range of piston speeds. There exists a specific piston speed at which the power delivered by the engine is maximum (P_{max}) and its corresponding efficiency is larger than half of the Carnot efficiency ($\frac{1}{2}\eta_c$). An optimization criterion leads to a trade-off between high power and high efficiency with respective values of $0.84P_{max}$ and $0.81\eta_c$. In addition, we found the time taken at the optimized state to be 1.67 times the time taken when operating at maximum power.

Chapter 1

Introduction

Nowadays, air pollution and global warming are serious issues threatening vegetation and wildlife on which man kind depends. The pollution produced by burning fuel from vehicles and industrial plants can also cause diseases such as asthma, cancer, heart and lung disease [1]. Designing more efficient engines is one possible way of reducing global warming and air pollution.

The efficiency of heat engines has been a basic subject of thermodynamics since the French scientist Nicolas Leonard Sadi Carnot derived the maximum efficiency of a reversible heat engine in 1824. Carnot showed that the efficiency of a reversible heat engine that works between hot and cold reservoirs at temperatures T_h and T_c, respectively, is given by (see Chapter 2 for the derivation)

$$\eta = 1 - \frac{T_c}{T_h}. \tag{1.0.1}$$

However, to obtain such a maximum efficiency, it takes an infinite amount of time to extract a finite amount of work. This means that the power delivered by the Carnot engine is zero and practically unimportant. Following Carnot's insight and since the industrial revolution, a lot of studies have been made concerning the efficiency of heat engines. The earliest study of efficiency at maximum power was done by Odum and Pikerton in 1955 [2]. Curzon and Ahlborn [3] calculated the efficiency of an endoreversible heat engine that operates at maximum power in 1975. Like the Carnot efficiency, the result obtained by

Curzon and Ahlborn depends only on the temperature of the reservoirs and is given by

$$\eta_{CA} = 1 - \sqrt{\frac{T_c}{T_h}}. \tag{1.0.2}$$

Many studies have been carried out regarding the efficiency of different heat engines that work at maximum power [4-8]. However; working at maximum power leads to substantial amount of the input energy to be wasted. On the other hand, working at maximum efficiency has no practical importance. Then one wonders how to make a trade off between maximum efficiency and maximum power. Let us make the idea behind more practical. Suppose you are driving your car so that the engine operates at maximum power. At this time the engine consumes high amount of fuel where a substantial amount of it being wasted. On the contrary, to use the fuel more efficiently and hence to save fuel expenditure, you want to drive as slow as possible, but at this point you realize that you are running out of time. In this work, we will use a criterion for the best compromise between maximum efficiency and maximum power for a heat engine.

A. Calvo Hernandez et al [9] proposed a unified optimization criterion for any energy converter: heat engine, heat pump or refrigerator. They proposed a criterion that gives best compromise between waste energy and effective energy. Our main goal in this thesis work is to find an (optimized) efficiency that lies between the maximum (Carnot) efficiency and the efficiency at maximum power for a process that operates at a finite time by using this optimization criterion. We considered a heat engine model originally studied by Y. Izumida and K. Okuda [10]. They used the model to make a numerical simulation on the validity of the Curzon-Ahlborn efficiency for the first time.

The material in this paper is arranged as follows. In Chapter two we will derive the efficiency of a reversible heat engines whose working material is ideal gas. In Chapter three we will present the optimization criterion proposed in [9] for a heat engine. In the fourth Chapter, we will see kinematics of hard spheres, the model taken for the study and

simulation techniques employed. The fifth Chapter is devoted to the results obtained by event-driven molecular dynamics simulation for quantities of our interest. In Chapter 6 we summarize the results and put the conclusions.

Chapter 2

Efficiency of a Reversible Heat Engine

Now we do the task of obtaining the efficiency of reversible heat engines. Since the efficiency of a reversible heat engine is the maximum, all of them must have the same form of efficiency. Hence obtaining the efficiency of one particular reversible engine will suffice. The following derivation also makes it explicit that the efficiency of Carnot's engine is only a function of temperature [1].

Carnot's reversible engine consists of an ideal gas that operates between a hot reservoir and a cold reservoir at temperatures T_h and T_c, respectively. A complete Carnot cycle consists of four processes. These are: isothermal expansion, adiabatic expansion, isothermal compression and adiabatic compression.

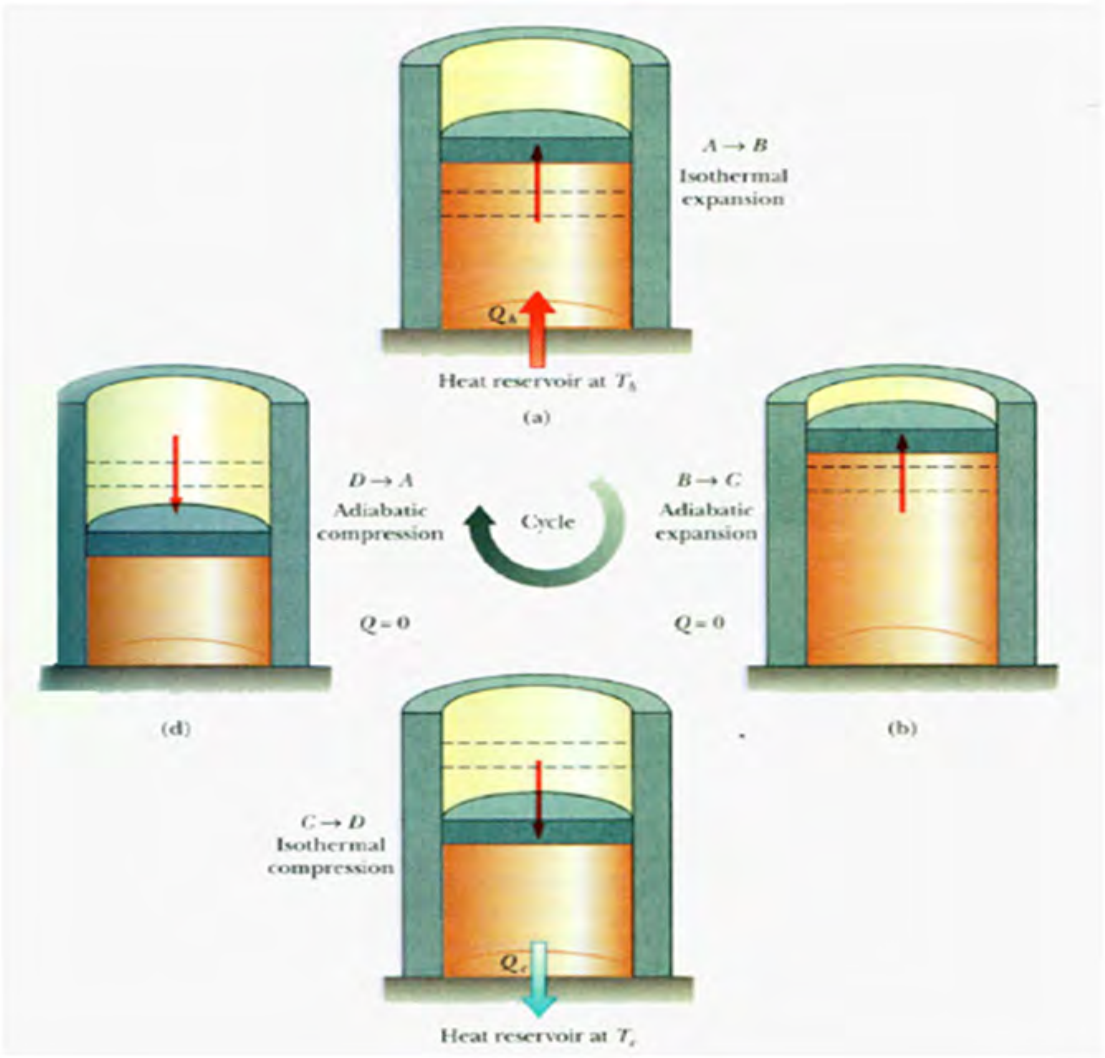

Figure 2.1: The four steps of Carnot cycle. From $(A \to B)$ and $(C \to D)$, the system is in contact with heat reservoir at temperature T_h and T_c, respectively, while it is insulated during steps $(B \to C)$ and $(D \to A)$

Fig. 2.1 above shows the four steps of Carnot's cycle. We look each step one by one as follows.

Step A: The gas has an initial volume V_A and is in contact with the hot reservoir at a temperature T_h. Staying in contact with the reservoir, the gas undergoes an infinitely slow reversible expansion to the state B, of volume V_B. During this process the work done by the gas is

$$W_{AB} = \int_{V_A}^{V_B} PdV. \tag{2.0.1}$$

Using the equation of state for an ideal gas (i.e. $PV = NK_BT$) and integrating, we obtain

$$W_{AB} = NK_BT_h \ln\left[\frac{V_B}{V_A}\right] \tag{2.0.2}$$

where N is the number of gas molecules and K_B is Boltzmann's constant. During this isothermal process, heat is absorbed from the hot reservoir. Since the internal energy of an ideal gas depends only on the temperature, there is no change in the energy of the gas; all the work done equals the heat absorbed. Hence the heat absorbed is

$$Q_{AB} = W_{AB}. \tag{2.0.3}$$

Step B: In the second step, the gas is thermally insulated from the reservoir; it is made to undergo an adiabatic expansion from state B to state C decreasing the temperature from T_h to T_c. During this adiabatic process, work is done by the gas. Noting that on the adiabatic from B to C we have

$$PV^\gamma = constant \tag{2.0.4}$$

where γ is the ratio of specific heat capacities of the working substance at constant pressure to that of at constant volume. The work done in this step is

$$W_{BC} = \int_{V_B}^{V_C} PdV = \int_{V_B}^{V_C} \frac{P_BV_B^\gamma}{V^\gamma}dV = \frac{P_CV_C - P_BV_B}{1-\gamma} \tag{2.0.5}$$

where we have used Eq. (2.0.4). Using the equation of state of an ideal gas, the above equation can be further simplified to obtain

$$W_{BC} = \frac{NK_B(T_h - T_C)}{\gamma - 1}. \tag{2.0.6}$$

Step C: In this third step, the gas is in contact with the reservoir of temperature T_c and undergoes an isothermal compression to the point D at which the volume V_D is such that an adiabatic compression can return it to the initial state A. During this process the work done can be obtained using similar procedure as **step A** and is given by

$$W_{CD} = NK_BT_c \ln\left[\frac{V_D}{V_C}\right]. \tag{2.0.7}$$

Step D: In this final step, an adiabatic compression takes the gas from state D to its initial state A. Since this process is similar to **step B**, we can write

$$W_{DA} = \frac{NK_B(T_c - T_h)}{\gamma - 1}. \tag{2.0.8}$$

The total work done in this reversible Carnot cycle is

$$W = W_{AB} + W_{BC} + W_{CD} + W_{DA} = Q_{AB} - Q_{CD} = NK_BT_h \ln\left[\frac{V_B}{V_A}\right] - NK_BT_c \ln\left[\frac{V_C}{V_D}\right]. \tag{2.0.9}$$

The efficiency(η), which is the ratio of the total work done to heat absorbed from the reservoir at temperature T_h is given by

$$\eta = \frac{W}{Q_{AB}} = 1 - \frac{NK_BT_c \ln\left[\frac{V_C}{V_D}\right]}{NK_BT_h \ln\left[\frac{V_B}{V_A}\right]}. \tag{2.0.10}$$

For the isothermal processes, we have $P_AV_A = P_BV_B; P_CV_C = P_DV_D$ and for the adiabatic processes, we have $P_BV_B^\gamma = P_CV_C^\gamma; P_DV_D^\gamma = P_AV_A^\gamma$. Using these relations, it can be easily seen that, $\frac{V_C}{V_D} = \frac{V_B}{V_A}$, and using this relation in Eq. (2.0.10), we arrive at a simple expression for the efficiency

$$\eta = 1 - \frac{T_c}{T_h}. \tag{2.0.11}$$

The efficiency in Eq. (2.0.11) is called the Carnot efficiency and it is the maximum possible value that can be attained for a given value of T_h and T_c.

Chapter 3

Optimization Criterion for Heat Engines

The two common efficiencies namely; the Carnot and Curzon-Ahlborn, were obtained for a process that results zero and maximum power respectively. As it can be seen from Eq. (1.0.1) and Eq. (1.0.2), the Curzon-Ahlborn efficiency obtained for a maximum power producing engine is smaller than that of the Carnot efficiency. To have more efficient engine, one may desire the Carnot engine type, but with side effect of powerlessness. On the contrary, to have a very power full engine, one may desire an engine that gives maximum power but less efficiency. In the case of optimized efficiency, one can obtain an efficiency that lies between the two extremes, (i.e between the maximum efficiency and the efficiency at maximum power) for a system that operates at a finite time. To accomplish this desired task, it is required to develop an objective function.

A. Calvo Hernandez et al [9] proposed an objective function for any energy converter, that gives the best compromise between useful energy and lost useful energy. Generally the choice of an objective function is at one's disposal but should obey the following three conditions. The first is, the dependence of the objective function on the parameters of the process should be a guidance in order to improve the performance of that process. The second criterion is, it should not depend on the parameters of the environment (that are not controllable). The third criterion is, it should take into account the unavoidable

dissipation of energy provoked by the process.

Let us consider an energy converter whose task is to produce a useful energy $E_u(x;\{\alpha\})$ by the conversion of an input energy $E_i(x;\{\alpha\})$ along a given non-ideal process. Here x denotes an independent variable while $\{\alpha\}$ denotes a set of parameters which can be considered as controls. The efficiency of this energy converter is the ratio of the useful energy to the input energy and is given by

$$\eta(x;\{\alpha\}) = \frac{E_u(x;\{\alpha\})}{E_i(x;\{\alpha\})}. \tag{3.0.1}$$

If we let $\eta_{min}(\{\alpha\})$ and $\eta_{max}(\{\alpha\})$ to be the minimum and maximum values of the efficiency respectively in the allowed values range of the variable x, we have

$$\eta_{min}(x;\{\alpha\}) \leq \eta(x;\{\alpha\}) \leq \eta_{max}(x;\{\alpha\}) \tag{3.0.2}$$

where

$$\eta_{min}(\{\alpha\}) = \frac{E_{u,min}(\{\alpha\})}{E_i(x;\{\alpha\})} \quad and \quad \eta_{max}(\{\alpha\}) = \frac{E_{u,max}(\{\alpha\})}{E_i(x;\{\alpha\})}. \tag{3.0.3}$$

For a given input energy, one has

$$\eta_{min}(\{\alpha\})E_i(x;\{\alpha\}) \leq E_u(x;\{\alpha\}) \leq \eta_{max}(x;\{\alpha\})E_i(x;\{\alpha\}). \tag{3.0.4}$$

These limits (i.e Eq. (3.0.2) and Eq. (3.0.4)) suggest to define an effective useful energy as

$$E_{u,eff}(x;\{\alpha\}) = E_u(x;\{\alpha\}) - \eta_{min}(\{\alpha\})E_i(x;\{\alpha\}) \tag{3.0.5}$$

and a lost useful energy as

$$E_{u,lost}(x;\{\alpha\}) = \eta_{max}(\{\alpha\})E_i(x;\{\alpha\}) - E_u(x;\{\alpha\}). \tag{3.0.6}$$

To obtain the best compromise between effective useful energy and lost useful energy, one introduces the Ω function as the difference between the quantities in Eq. (3.0.5) and Eq.

(3.0.6), i.e

$$\Omega(x;\{\alpha\}) = E_{u,eff}(x;\{\alpha\}) - E_{u,lost}(x;\{\alpha\}) = 2E_u(x;\{\alpha\}) - [\eta_{min}(\{\alpha\}) + \eta_{max}(\{\alpha\})]E_i(x;\{\alpha\}). \tag{3.0.7}$$

Substituting the value of $E_i(x;\{\alpha\})$ from Eq. (3.0.1), one obtains

$$\Omega(x;\{\alpha\}) = \frac{2\eta(x;\{\alpha\}) - [\eta_{min}(\{\alpha\}) + \eta_{max}(\{\alpha\})]}{\eta(x;\{\alpha\})} E_u(x;\{\alpha\}). \tag{3.0.8}$$

The rate dependence of Eq. (3.0.8) is given by

$$\dot{\Omega}(x;\{\alpha\}) = \frac{2\eta(x;\{\alpha\}) - [\eta_{min}(\{\alpha\}) + \eta_{max}(\{\alpha\})]}{\eta(x;\{\alpha\})} \dot{E}_u(x;\{\alpha\}). \tag{3.0.9}$$

where the dot over $E_u(x;\{\alpha\}$ and $\Omega(x;\{\alpha\})$ denotes the time derivative. Equation (3.0.9) is the objective function that identifies the optimum path that gives the best compromise between effective useful energy and lost useful energy [9]. In Chapter 5, we will use this equation to identify the value of the control parameter (x) that gives optimum performance for the heat engine model we considered.

Chapter 4

Model and Simulations

In this chapter we will present the model considered as a heat engine as well as simulation techniques employed. First, we look at the kinematics of hard spheres. Since we have used an ideal gas as a working substance, a discussion about the kinematics of hard spheres is important. Specifically, we will discuss on the necessary and sufficient conditions for two hard spheres to collide, if so when will they collide and their post collision velocities will be calculated. Then we will present a brief description of the heat engine model as well as simulation techniques carried out.

4.1 Kinematics of Hard-Sphere Collisions

Molecular dynamics algorithms are divided into two broad classes [12]: those for soft bodies, for which the intermolecular forces are continuous functions of the distance between molecules and those for hard bodies for which the forces are discontinuous. For hard bodies the discontinuity in the force extends to the intermolecular potential; in particular, hard spheres of diameter σ interact through a potential energy function $U(r)$ of the form

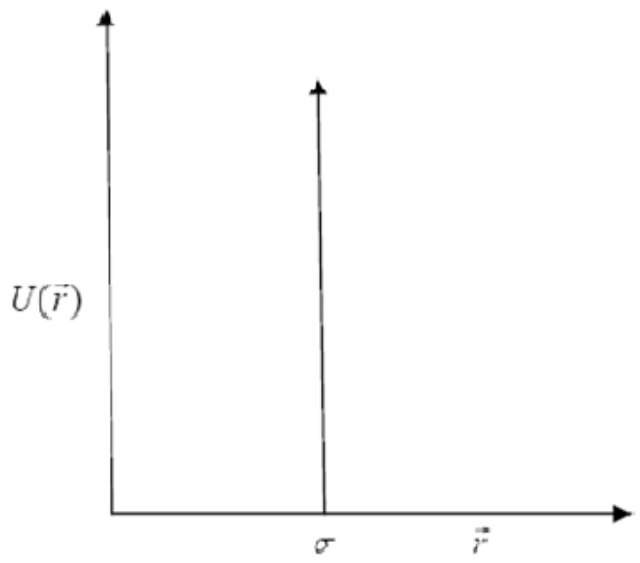

Figure 4.1: The pair potential energy function $U(r)$ for hard spheres of diameter σ. Two spheres exert no force unless they collide [12].

$$U(x) = \begin{cases} \infty & , \quad r \leq \sigma, \\ 0 & , \quad r > \sigma. \end{cases} \tag{4.1.1}$$

Thus, hard spheres exert forces on one another only when they collide. Between collisions the spheres travel along straight lines at constant velocities, and so, rather than computing the trajectories, the simulation algorithm computes the times of collisions. The calculation is purely algebraic because collisions are taken to be perfectly elastic: during a collision no energy is transferred either to deform a sphere or to change its internal state. Hence, collisions disrupt neither conservation of linear momentum nor conservation of kinetic energy, and these two principles enable us to determine collision times.

Consider two hard spheres having equal masses ($m_1 = m_2 = m$) and equal diameters ($\sigma_1 = \sigma_2 = \sigma$), with their motion constrained to one dimension. At some time t_1 these spheres are separated by a distance x and have velocities $\vec{v}_{01}$ and $\vec{v}_{02}$ such that they will collide at some latter time $t_2 > t_1$. Now at time t_1 no forces are acting on the spheres;

hence, by Newton's first law, $\vec{v}_{01}$ and $\vec{v}_{02}$ are constants. Our immediate objective is to determine the velocities $\vec{v}_{f1}$ and $\vec{v}_{f2}$ after the collision at t_2. Conservation of linear momentum gives

$$m\vec{v}_{01} + m\vec{v}_{02} = m\vec{v}_{f1} + m\vec{v}_{f2} \tag{4.1.2}$$

or

$$\vec{v}_{01} + \vec{v}_{02} = \vec{v}_{f1} + \vec{v}_{f2}. \tag{4.1.3}$$

Conservation of energy gives

$$\frac{1}{2}m\vec{v}_{01}^2 + \frac{1}{2}m\vec{v}_{02}^2 = \frac{1}{2}m\vec{v}_{f1}^2 + \frac{1}{2}m\vec{v}_{f2}^2 \tag{4.1.4}$$

or

$$\vec{v}_{01}^2 + \vec{v}_{02}^2 = \vec{v}_{f1}^2 + \vec{v}_{f2}^2. \tag{4.1.5}$$

From Eq. (4.1.3) and Eq. (4.1.5) we get

$$\vec{v}_{f1} = \vec{v}_{02} \quad \textit{and} \quad \vec{v}_{f2} = \vec{v}_{01}. \tag{4.1.6}$$

Thus for purely one-dimensional motions, a perfectly elastic collision between spheres of equal masses cause the two spheres to exchange velocities.

Our interest here is in using the one-dimensional result in Eq. (4.1.6) to deduce the kinematics of hard-sphere collisions in two and three dimensions. In any space-one, two, or three dimensions-when hard spheres collide, the repulsive force is exerted along the line of sphere centers $\vec{r}_{12} = \vec{r}_2 - \vec{r}_1$: only components of the velocities parallel to $\vec{r}_{12}$ are affected by a perfectly elastic collision. Thus, we define a set of mutually orthogonal axes $\{\hat{r}_{12}, \hat{j}, \hat{k}\}$, where the carets denote unit vectors: $\hat{r}_{12} = \frac{\vec{r}_{12}}{|\vec{r}_{12}|}$. The pre-collision velocity of sphere i can be written as

$$\vec{v}_{0i} = (\vec{v}_{0i}.\hat{r}_{12})\hat{r}_{12} + (\vec{v}_{0i}.\hat{j})\hat{j} + (\vec{v}_{0i}.\hat{k})\hat{k} \tag{4.1.7}$$

and the post collision velocity can be written as

$$\vec{v}_{fi} = (\vec{v}_{fi}.\hat{r}_{12})\hat{r}_{12} + (\vec{v}_{fi}.\hat{j})\hat{j} + (\vec{v}_{fi}.\hat{k})\hat{k}. \tag{4.1.8}$$

Now, from our one-dimensional results (4.1.6), we expect that, on collision of spheres 1 and 2 components of $\vec{v}_1$ and $\vec{v}_2$ parallel to $\vec{r}_{12}$ will be exchanged:

$$\vec{v}_{f1}.\hat{r}_{12} = \vec{v}_{02}.\hat{r}_{12} \tag{4.1.9}$$

$$\vec{v}_{f2}.\hat{r}_{12} = \vec{v}_{01}.\hat{r}_{12} \tag{4.1.10}$$

while components perpendicular to $\vec{r}_{12}$ are unaffected:

$$\vec{v}_{f1}.\hat{j} = \vec{v}_{01}.\hat{j}, \qquad \vec{v}_{f2}.\hat{j} = \vec{v}_{02}.\hat{j}, \qquad \vec{v}_{f1}.\hat{k} = \vec{v}_{01}.\hat{k}, \qquad \vec{v}_{f2}.\hat{k} = \vec{v}_{02}.\hat{k}. \tag{4.1.11}$$

Using Eq. (4.1.9) and Eq. (4.1.11) we get for particle 1

$$\vec{v}_{f1} = (\vec{v}_{01}.\hat{r}_{12})\hat{r}_{12} + (\vec{v}_{01}.\hat{j})\hat{j} + (\vec{v}_{01}.\hat{k})\hat{k}. \tag{4.1.12}$$

Subtracting the initial velocity of particle 1 from its final velocity in (4.1.8), we obtain

$$\vec{v}_{f1} = \vec{v}_{01} + [(\vec{v}_{02} - \vec{v}_{01}).\hat{r}_{12}]\hat{r}_{12}. \tag{4.1.13}$$

The analogous procedure for sphere 2 gives

$$\vec{v}_{f2} = \vec{v}_{02} + [(\vec{v}_{01} - \vec{v}_{02}).\hat{r}_{12}]\hat{r}_{12}. \tag{4.1.14}$$

Equations (4.1.13) and (4.1.14) give the post-collision velocities in terms of the (known) pre-collision velocities $\vec{v}_{0i}$.

4.1.1 Collision Times

Before applying equations (4.1.13) and (4.1.14), we must determine whether spheres 1 and 2 will collide and, if so when. In this section we first describe the calculation of collision times for any two spheres. Consider two spheres, 1 and 2, each having diameter σ. When they collide, the centers of 1 and 2 will be separated by diameter σ; that is

$$|\vec{r}_1(t_c) - \vec{r}_2(t_c)| = \sigma \tag{4.1.15}$$

where t_c is the time at which collision occurs. Between collisions, the spheres transverse straight lines at constant velocities; so from the (known) initial position $\vec{r}_0(t)$, the position of sphere i at any latter time t is

$$\vec{r}_i(t) = \vec{r}_i(t_0) + (t - t_0)\vec{v}_{0i}(t_0). \tag{4.1.16}$$

Using (4.1.16) in (4.1.15) for $\vec{r}_1$ and $\vec{r}_2$ produces a quadratic for the collision time t_c

$$|\vec{r}_{12} + (t_c - t_0)\vec{v}_{12}|^2 = \sigma^2 \tag{4.1.17}$$

where $\vec{r}_{12} = \vec{r}_1(t_0) - \vec{r}_2(t_0)$ and $\vec{v}_{12} = \vec{v}_1(t_0) - \vec{v}_2(t_0)$.

The solution of the quadratic (4.1.17) is

$$t_c = t_0 + \frac{-\vec{v}_{12}.\vec{r}_{12} \pm [(\vec{v}_{12}.\vec{r}_{12})^2 - \vec{v}_{12}^2(\vec{r}_{12}^2 - \sigma^2)]^{\frac{1}{2}}}{\vec{v}_{12}^2} \tag{4.1.18}$$

Equation (4.1.18) contains all the possibilities regarding an encounter between spheres 1 and 2. Specifically, it allows us to distinguish three important situations.

Situation A:

$$\vec{v}_{12}.\vec{r}_{12} < 0 \tag{4.1.19}$$

for collision. The product $\vec{v}_{12}.\vec{r}_{12}$ is proportional to the component of the velocity difference along the line of centers. If this component is negative, then the spheres are approaching one another and a collision may occur.

Situation B:

$$(\vec{v}_{12}.\vec{r}_{12})^2 - \vec{v}_{12}^2(\vec{r}_{12}^2 - \sigma^2) \geq 0 \tag{4.1.20}$$

for collision.

Equation (4.1.19) is only a necessary, not a sufficient, condition for a collision; that is the spheres may move towards one another but still not collide. A sufficient condition for collision is provided by Eq. (4.1.20), for which a geometric interpretation is given in Fig. 4.2.

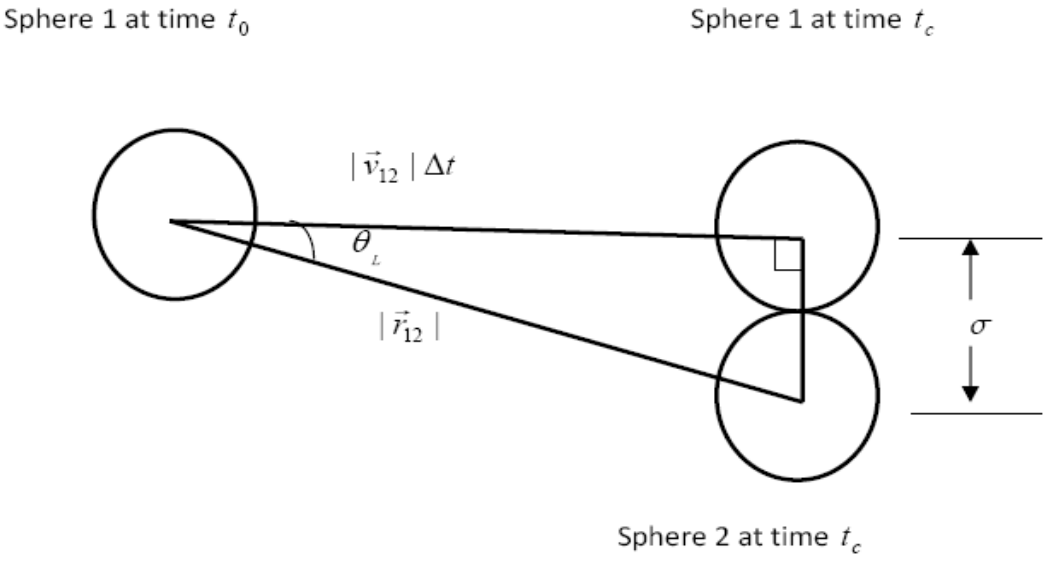

Figure 4.2: Geometric interpretation of the discriminant in (2.2.4) showing the largest value of angle θ for which spheres 1 and 2 collide. This limiting value of the angle of approach occurs when the triangle $\{|\vec{v}_{12}|\Delta t, |\vec{r}_{12}|, \sigma\}$ is right angle [12].

To prove (4.1.20), we proceed as follows. In figure 4.2 the relative velocity $\vec{v}_{12}$ prescribes the trajectory of sphere 1 relative to 2. When sphere 1 and 2 collide at time t_c, the angle between $\vec{v}_{12}$ and $\vec{r}_{12}$ must be less than or equal to the largest angle, θ_L. Thus, for collision to occur

$$cos\theta \ \geq cos\theta_L. \tag{4.1.21}$$

But from the right triangle in Fig. 4.2 we have

$$cos\theta_L = \frac{|\vec{v}_{12}|\Delta t}{|\vec{r}_{12}|} \tag{4.1.22}$$

$$(|\vec{v}_{12}|\Delta t)^2 = |\vec{r}_{12}|^2 - \sigma^2 \tag{4.1.23}$$

where Δt is $t_c - t_0$. Rearranging and squaring (4.1.22)

$$|\vec{r}_{12}|^2 cos^2\theta \geq |\vec{v}_{12}|\Delta t^2 \tag{4.1.24}$$

and using (4.1.23) we get

$$\vec{r}_{12}^2 \cos^2\theta > \vec{r}_{12}^2 - \sigma^2. \tag{4.1.25}$$

Multiplying both sides of (4.1.25) by $\vec{v}_{12}^2$ and rearranging we get

$$(\vec{v}_{12}.\vec{r}_{12})^2 - \vec{v}_{12}^2(\vec{r}_{12}^2 - \sigma^2) \geq 0 \tag{4.1.26}$$

which is the sufficient condition for collision to occur between spheres 1 and 2.

Situation C: when the condition (4.1.20) is satisfied, the quadratic (4.1.17) has two roots. These roots imply that, for a given separation $\vec{r}_{12}$ and relative velocity $\vec{v}_{12}$ leading to a collision, two geometric arrangements have the spheres in contact, as shown in Fig. 4.3 below.

Since the spheres are impenetrable, only the short time root (negative sign in (4.1.18)) is physically possible. In the case of grazing contact, the discriminant is zero, the equality in (4.1.20) applies, and the quadratic (4.1.17) has a single root.

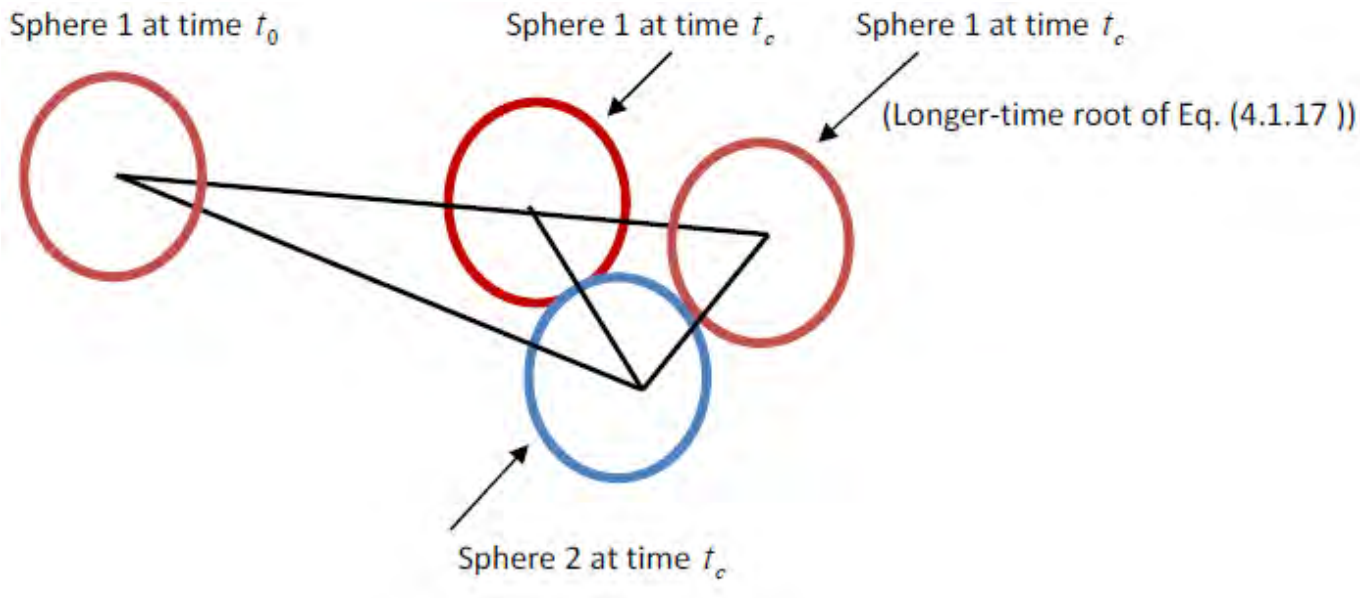

Figure 4.3: Geometric interpretation of the two roots of the quadratic (4.1.17). For given $\vec{r}_{12}$ and $\vec{v}_{12}$ there are two geometric arrangements that have spheres 1 and 2 in contact, but for impenetrable spheres only the short-time root is physically possible [12].

4.2 Model

We consider the quasi-static Carnot cycle gas (as discussed in Chapter1) . For simplicity, we here use the two dimensional model. This model is originally developed and used by Y. Izumida and K. Okuda [10]. They used the model to test the validity of the Curzon-Ahlborn efficiency [2] using numerical experiments. The usual quasi-static Carnot cycle of an ideal gas consists of four processes: (A): isothermal expansion process ($V_1 \to V_2$), (B): adiabatic expansion process ($V_2 \to V_3$), (C): isothermal compression process($V_3 \to V_4$), (D): adiabatic compression process ($V_4 \to V_1$) where V_i's are the volumes of the cylinder at which we switch each of the four processes (Fig. 4.4a). When we fix T_h, T_c, V_1, and V_2 we can easily determine the volumes V_3, and V_4 since we assume an ideal gas as the working substance. For a quasi-static process that uses an ideal gas as a working substance, we have the relation $TV^{\gamma-1} = constant$ for the adiabatic processes. Here γ refers to the ratio of the specific heat capacity at constant pressure to that at constant volume. For a two dimensional ideal gas γ is 2. Therefore, $V_3 = (T_h/T_c)V_2$ and $V_4 = (T_h/T_c)V_1$ for the two dimensional case. In the case of finite-time cycle, we assume that the right wall of the cylinder is a piston and moves back and forth at a constant speed u. In this model, this u is taken as a unique parameter, which is a controllable parameter. We also assume that each process is switched at the same volume as in the quasi-static case.

4.3 Simulation

We have performed the two-dimensional event-driven molecular dynamics simulation as follows. We assume N hard-disc particles of diameter d and mass m, which are confined into the two dimensional cylinder with rectangular geometry and the collision between hard-disc particles are perfectly elastic. Defining (x, y) coordinates as in Fig. 4.4b, we let the piston move along the x-axis at a finite constant speed u. Here, we express the

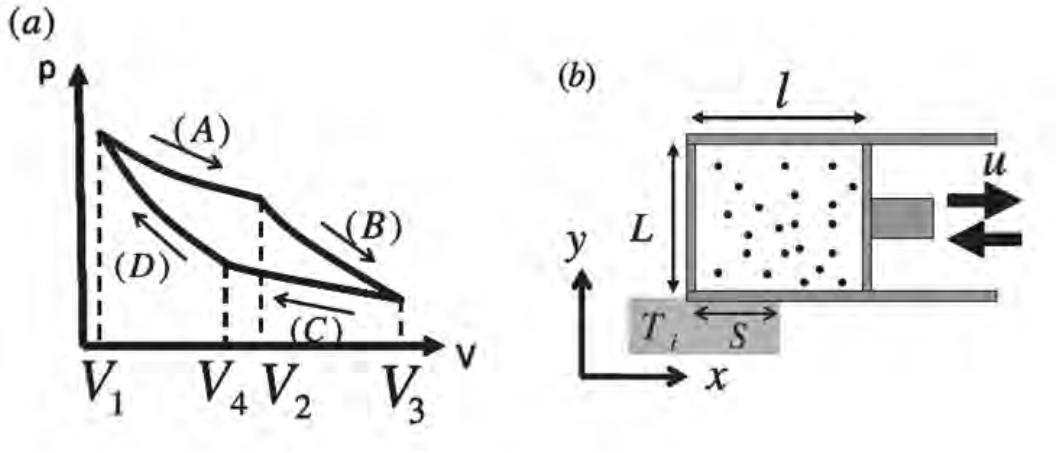

Figure 4.4: Schematic illustration of the model. (a) Pressure-volume $(P - V)$ diagram of a quasi-static Carnot cycle for an ideal gas. (b) The piston moves at a finite constant speed u and the thermalizing wall with temperature $T_i (i = h, c)$ and the length S is set on the left bottom of the cylinder only in the isothermal processes [10].

x-length and the y-length of the cylinder as l and L, respectively. Then the volume V_i $(i = 1, ...4)$ of the cylinder at which we switch each of the four processes (Fig. 4.4a) becomes $V_i = Ll_i$, where l_i is the x-length of the cylinder at the switching volume V_i. If the process (A) begins at time t=0, then the volume $V(t)$ of the cylinder at time t is given as

$$V(t) = Ll(t) = L(ut + l_1) \qquad for \qquad 0 \leq t \leq \frac{(l_3 - l_1)}{u}, \tag{4.3.1}$$

in the expansion processes (A) and (B). and

$$V(t) = L(-ut + 2l_3 - l_1) \qquad for \qquad \frac{(l_3 - l_1)}{u} \leq t \leq \frac{2(l_3 - l_1)}{u} \tag{4.3.2}$$

in the compression processes (C) and (D).

Let us now investigate the collision of particles with the moving piston. To do so, we classify collision of a particle with the piston into two categories: (i) piston moving forward (expansion process) and (ii) piston moving backwards (compression process).

(I) **Piston moving forward**

During this process, if a particle is to collide with the piston its x-velocity must be to the right and must have larger magnitude than that of the pistons speed u. Denote v_{0x}, v_{fx}

and u_f the initial speed, final speed of the particle and final speed of the moving piston respectively. Conservations of linear momentum and kinetic energy give the relations

$$mv_{0x} + Mu = mv_{fx} + Mu_f, \tag{4.3.3}$$

and

$$\frac{1}{2}mv_{0x}^2 + \frac{1}{2}Mu^2 = \frac{1}{2}mv_{fx}^2 + \frac{1}{2}Mu_f^2, \tag{4.3.4}$$

where m and M are mass of the particle and piston respectively. From these equations we obtain the relation

$$v_{fx} = u + u_f - v_{0x}. \tag{4.3.5}$$

Since we assume that the mass of the piston is very large compared to the mass of the colliding particle, (i.e $M \gg m$), the speed of the piston does not change appreciably due to collision with a single particle. Therefore, the final speed of a colliding particle with the piston becomes

$$v_{fx} \approx 2u - v_{0x}. \tag{4.3.6}$$

The change in kinetic energy (ΔKE) of a colliding particle, which is the difference between its final and initial kinetic energies, is

$$\Delta KE = \frac{1}{2}m(v_{fx}^2 - v_{0x}^2) = 2mu(u - v_{0x}). \tag{4.3.7}$$

Since v_{0x} must be greater than u, Eqn. (4.3.7) tells us that the colliding particle loses energy, thereby transferring it to the forwardly moving piston.

(II) **Piston moving backward**

When the piston is moving backwards (compression process) there are two situations that a particle collision with the piston may occur. The first and obvious one is when a particle moves to the right. The second is that, while a particle moves to the left, collision occurs as long as the speed of the piston is greater than that the particle. We will see both cases as follows.

If a particle moves to the negative x-axis, the laws of momentum and energy conservations can be written as

$$-mv_{0x} - Mu = -mv_{fx} - Mu_f \tag{4.3.8}$$

and

$$\frac{1}{2}mv_{0x}^2 + \frac{1}{2}Mu^2 = \frac{1}{2}mv_{fx}^2 + \frac{1}{2}Mu_f^2. \tag{4.3.9}$$

Again, using the fact that the mass of the piston is very large compared to a colliding particle, the final speed of a colliding particle obtained from the above two equations is

$$v_{fx} \approx -(2u + v_{0x}) \tag{4.3.10}$$

and the corresponding change in the particle's kinetic energy is

$$\Delta KE = 2mu(u + v_{0x}). \tag{4.3.11}$$

If a particle moves towards the positive x-axis, again using the laws of conservation of linear momentum and kinetic energy, we find that the final speed of a colliding particle is

$$v_{fx} \approx -(v_{0x} + 2u) \tag{4.3.12}$$

and the corresponding change in kinetic energy is

$$\Delta KE = 2mu(u + v_{0x}). \tag{4.3.13}$$

Thus, from the above discussions, if a particle with the velocity $\vec{v}_0 = (v_x, v_y)$ collides with the piston whose x-velocity is $\pm u$, its velocity changes to $\vec{v}_f = (-v_x \pm 2u, v_y)$. Therefore, the particle does microscopic work of amount $m(|\vec{v}|^2 - |\vec{v}_f|^2)/2 = 2m(\pm uv_x - u^2)$ against the piston.

For the isothermal processes, to simulate the heat reservoirs, we set the thermal wall at desired temperature with the length S at the left bottom of the cylinder (see Fig. 4.4b).

The thermal wall has the following feature: When a particle collides with the thermal wall, its velocity stochastically changes to the value governed by the distribution function

$$f(\vec{v}, T_i) = \frac{1}{\sqrt{2\pi}} \left(\frac{m}{k_B T_i}\right)^{\frac{3}{2}} v_y \exp\left(\frac{-m\vec{v}^2}{2k_B T_i}\right) \tag{4.3.14}$$

$(-\infty < v_x < +\infty, 0 < v_y < +\infty, T_i \ (i = h \quad \text{in (A)}, \ c \quad \text{in(C)}))$, where k_B is Boltzmann constant. This thermal wall may be understood as follows [10]. Imagine a large particle reservoir thermalized at a temperature $T_i (i = h \text{ or } c)$ instead of the thermal wall and assume that if a particle in the cylinder goes out into the particle reservoir, another particle from the particle reservoir enters into the cylinder. From this consideration, we can see that the particle entering in to the cylinder from the particle reservoir obeys the velocity distribution function proportional to the Boltzmann factor multiplied by v_y. By normalizing, we obtain the distribution function Eqn.(4.3.14). This thermalizing wall guarantees that the particle velocities in the static system are governed by Maxwell-Boltzmann distribution with temperature T_i:

$$f_{MB}(\vec{v}, T_i) \equiv \frac{m}{2\pi k_B T_i} \exp\left(\frac{-m\vec{v}^2}{2k_B T_i}\right) \tag{4.3.15}$$

The heat flowing from the thermalizing wall into the system can microscopically be calculated by the difference between the kinetic energies before and after the collision with the thermal wall. We sum up the above microscopic heat during the simulation as well as the microscopic work. At the walls except for the piston and the thermal wall, we adopt the reflecting boundary condition for colliding particles. We have used N=100 particles with diameter, d=0.01 and mass, m=1 in the system with L=1, l_1=1, l_2=1.5, T_h=1, T_c=0.7, k_B=1 and length of the reservoir, S=0.5.

To perform the simulation, we have developed a Fortran 90 program that can do the task of the engine discussed above. The simulation technique used is event driven molecular dynamics, i.e we are interested at particular times at which collision occurs either for a particle with another particle or a particle with the boundaries of the container. The time at which particle to particle collision occurs is calculated according to equation (4.1.18)

with the negative sign. Particle collision with the container boundaries are calculated as follows. Let t_x and t_y denote the collision times with the boundaries perpendicular to the x and y axes respectively. There are two boundaries that are perpendicular to the y-axis, the bottom and top sides of the cylinder. Similarly we have two boundaries perpendicular to the x-axis, the left side of the cylinder and the moving piston.The collision time for the particle i with the x-boundary is given by

$$t_{xi} = \frac{x_{fi} - 0.5d - x_{0i}}{v_{xi}} \tag{4.3.16}$$

for v_{xi} is greater than zero and

$$t_{xi} = \frac{0.5d - x_{0i}}{v_{xi}} \tag{4.3.17}$$

for v_{xi} is less than zero. Note that v_{xi} is the initial speed of particle i and x_{0i} and x_{fi} are the initial and final x-positions respectively for that particle. A similar expression for t_{yi} is given by;

$$t_{yi} = \frac{L - 0.5d - y_{0i}}{v_{yi}} \tag{4.3.18}$$

for v_{yi} is greater than zero and

$$t_{yi} = \frac{0.5d - y_{0i}}{v_{yi}} \tag{4.3.19}$$

for v_{yi} is greater than zero. Since there is no moving boundary in the y-direction, unlike the final x -position, here we always have a fixed y-position L.

During the simulation procedure, we have tabulated all possible collision times. Once having the collision times, the next step is to identify the least collision time as well as to which particle (or a pairs of particles) does this minimum time belongs to. Then all particles positions are updated according to linear motion at constant velocity. For a colliding particle (particles, if a collision happens between a pair), we have updated the velocities according to the laws of elastic collision. The amount of net work done is calculated as the difference between the work done by the colliding particle on the moving piston during the expansion process and the work done by the piston on the particles during the the compression process. The total input heat is obtained by calculating the

change in kinetic energy of particles entering in to the thermal wall. Taking the ratio of the net work done to that of the total input heat, we calculated the efficiency of the engine. The power is also calculated by taking the ratio of the network done to that of the total time.

Chapter 5

Results and Discussion

5.1 Results

We had performed the two-dimensional event-driven molecular dynamics simulation, and calculated the averaged quantities, such as temperature of the working substance as a function of volume, efficiency and power as a function of piston speed which is our control parameter. We had calculated these quantities as the average over a certain number of complete cycles depending on the speed of the piston, in such a way that almost equal time is elapsed to obtain a value of the desired averaged quantity for each value of piston speed. If we let W_i and Q_{Hi} to be the amount of work done and heat absorbed during the i^{th} cycle respectively, then the average work done ($\overline{W}$) and the average heat ($\overline{Q}_H$) are given respectively by

$$\overline{W} = \frac{\sum_{i=n+1}^{N_c} W_i}{N_c - n}, \tag{5.1.1}$$

and

$$\overline{Q}_H = \frac{\sum_{i=n+1}^{N_c} Q_{Hi}}{N_c - n}, \tag{5.1.2}$$

where N_c is the number of cycles that the engine completed and n is the number of cycles that the engine performed to "warm up" before any data is being recorded. The average efficiency of our heat engine defined as the ratio of the average work done to the average

heat absorbed, is then given by

$$\overline{\eta} = \frac{\overline{W}}{\overline{Q}_H} = \frac{\sum_{i=n+1}^{N_c} W_i}{\sum_{i=n+1}^{N_c} Q_{Hi}}. \tag{5.1.3}$$

We had also calculated the average power as the ratio of the average work done to the total time elapsed for $N_c - n$ cycles. The time taken by the engine to perform a single cycle is fixed by the piston speed u whose value is $\frac{2(l_3-l_1)}{u}$. The total time elapsed to make many complete cycles is thus a multiple of this value. The average power for $N_c - n$ cycles is calculated as

$$\overline{P} = \frac{u}{2(N_c - n)(l_3 - l_1)} \sum_{i=n+1}^{N_c} W_i. \tag{5.1.4}$$

We have plotted temperature versus volume diagram for both the quasi-static and finite time results. The quasi-static plot is obtained by setting a constant temperature of 1.0 for the isothermal expansion stage and 0.7 for the isothermal compression stage, while for the adiabatic stages, we solved the equation $TV^{\gamma-1} = constant$ numerically. For the molecular dynamics simulation, we summed up the kinetic energy of all the particles and used the principle of equipartition theorem to calculate the temperature.

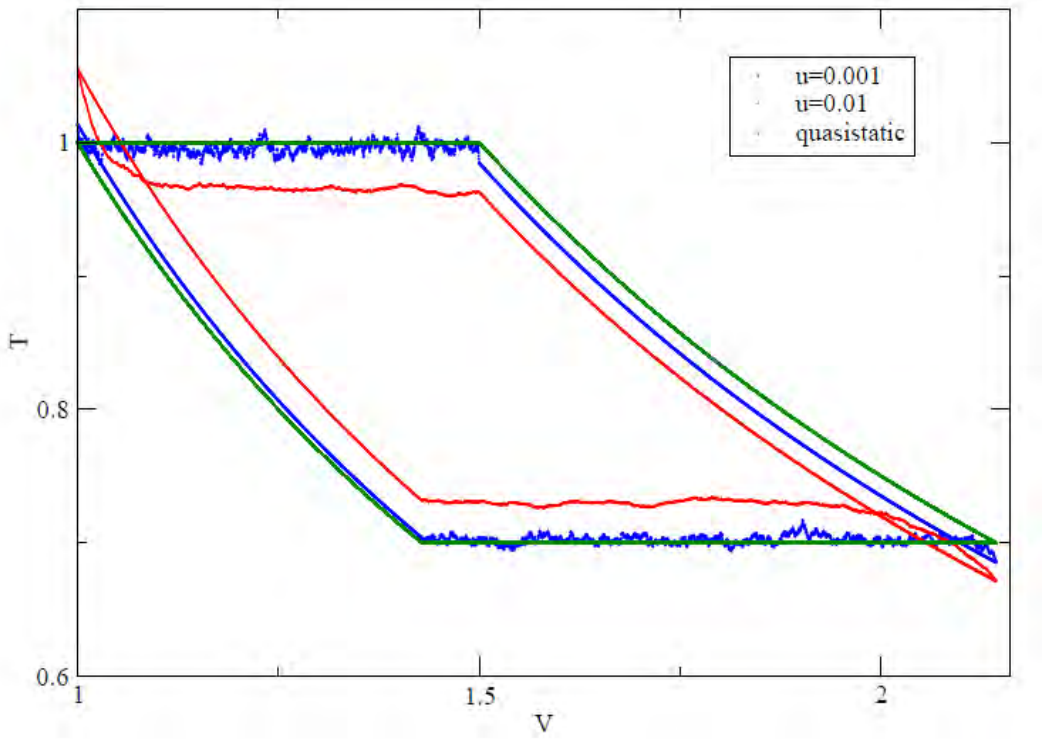

Figure 5.1: Temperature(T) versus volume(V) graph. Green: quasi-static result, Blue: finite time with u = 0.001, Red: finite time result with u = 0.01

As we can see from the plots of Fig. 5.1, as the speed of the piston gets very small, the molecular dynamics simulation result approaches to that of the quasi-static result. Generally, the molecular dynamics result deviates from the quasi-static result. This result ensures that the model can describe the ideal gas model heat engine to a good accuracy. We now present the plots of the average efficiency and average power as a function of the piston speed.

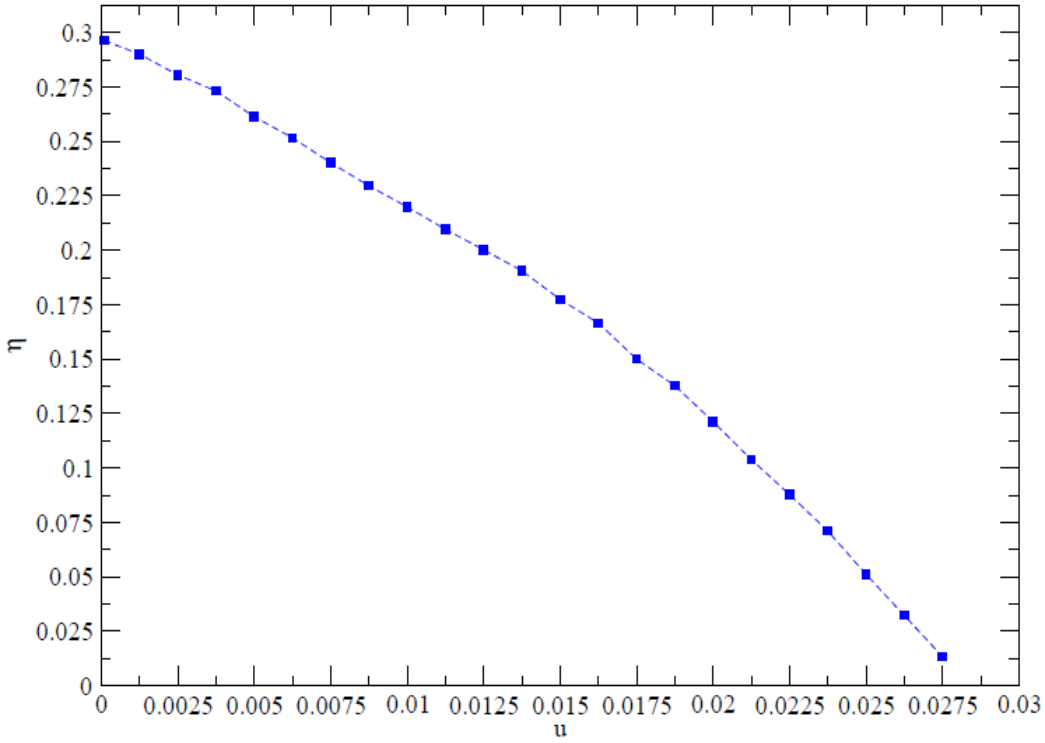

Figure 5.2: Average efficiency as a function of piston speed. The data is obtained by averaging over 14 - 3667 cycles after 1-46 "warming up" cycles, depending on the value of the piston speed.

Figure 5.2 above represents the way efficiency varies with piston speed. The Carnot efficiency is very well realized for small piston speed values. The average efficiency is in fact obtained to be 0.296 for piston speed value of 0.0001. Since we had taken T_h and T_c to be 1.0 and 0.7 respectively, the corresponding Carnot efficiency is 0.3.

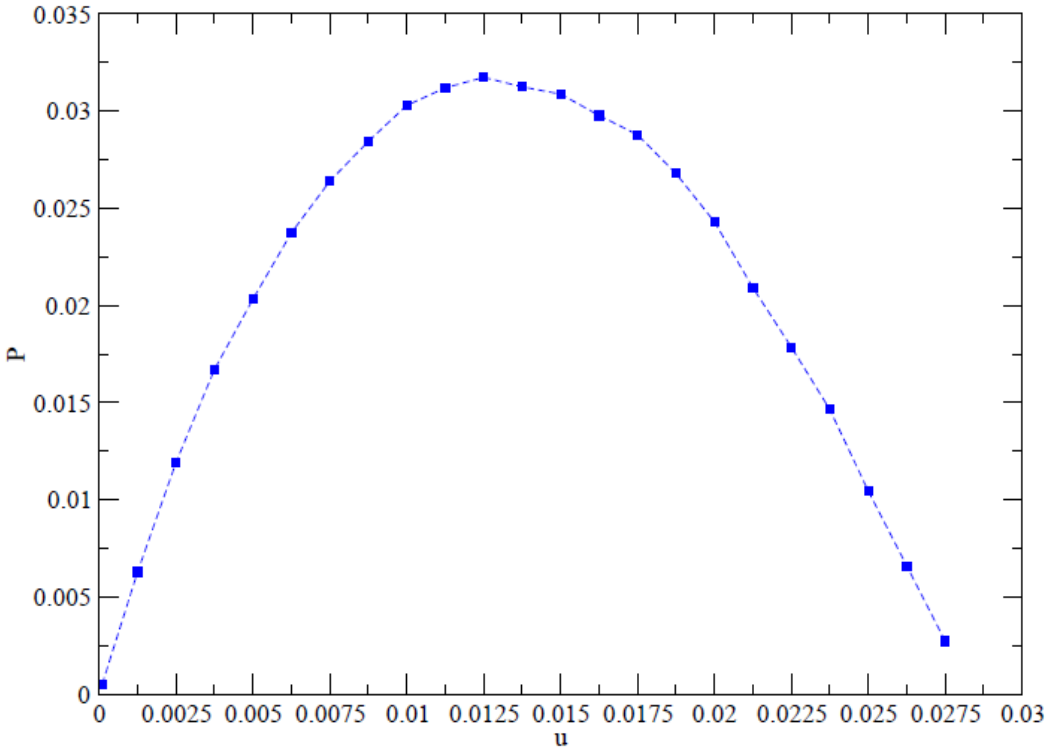

Figure 5.3: Average power as a function of piston speed. The data is obtained by averaging over 14 - 3667 cycles after 1-46 "warming up" cycles, depending on the value of the piston speed. The power is maximum at 0.0125.

As it can be seen from the graph in Fig. 5.3, the average power exhibits a maximum value. The efficiency at maximum power is obtained to be 0.199 ± 0.002 and is greater than the corresponding Curzon-Ahlborn efficiency [2] which takes a value of 0.163 for the given values of T_h and T_c. Another feature of the result is that the power vanishes when the process becomes very slow as well as when it is very fast. The reason is that although there is a finite amount of work done for a vanishingly small piston speed value, the time taken is so very large that the power becomes vanishingly small. Similarly, when the process is speeded up, the net average work done is very small even if the time per cycle is also small and the net outcome is a vanishingly small value of average power.

To obtain the optimized efficiency, we have used the data obtained for the efficiency as well as the power as a function of piston speed and used it in equation (3.0.9). We had used two ways of obtaining the optimized efficiency. In the first case we have considered

the entire range of the control parameter (piston speed). In this case we take the maximum efficiency to be the Carnot efficiency and the minimum efficiency to be zero. In the second case we have taken the minimum efficiency to be that of the efficiency at the maximum power, i.e 0.199, while the maximum efficiency as in the first case is taken to be the Carnot efficiency. Fig. 5.4 is a plot of the objective function as a function of the piston speed when we consider the entire parameter value range.

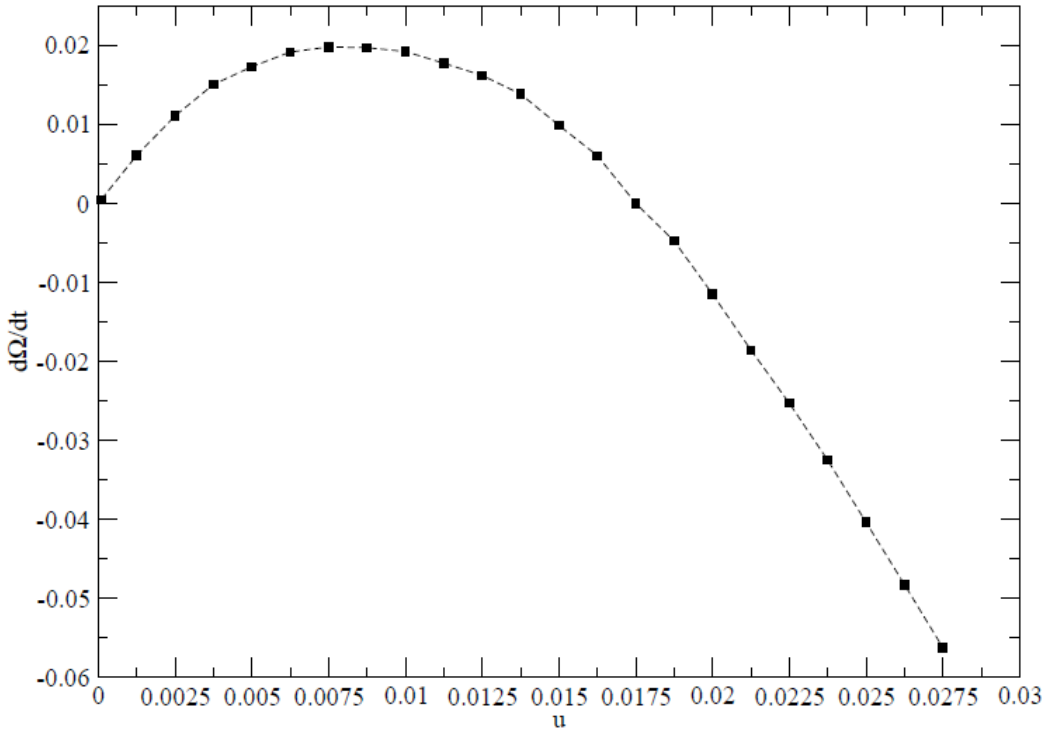

Figure 5.4: Objective function as a function of piston speed obtained in the entire range of piston speed values. The function attains its maximum at 0.0075.

The objective function attains its maximum value when it takes the value of piston speed of 0.0075. For this value of piston speed, we have obtained the (optimized) efficiency to be 0.242 ± 0.002. This efficiency lies between 0.30 and 0.199 which are the Carnot efficiency and the efficiency at maximum power respectively and is equivalent to $0.81\eta_c$. The power that the engine can deliver when working at this speed is $0.84P_{max}$, where P_{max} is the maximum power.

Now let us see the plot of the objective function we find in the second case, i.e the optimized efficiency obtained by taking the minimum efficiency to be that of the efficiency at maximum power. The plot for the objective function is shown in Fig. 5.5.

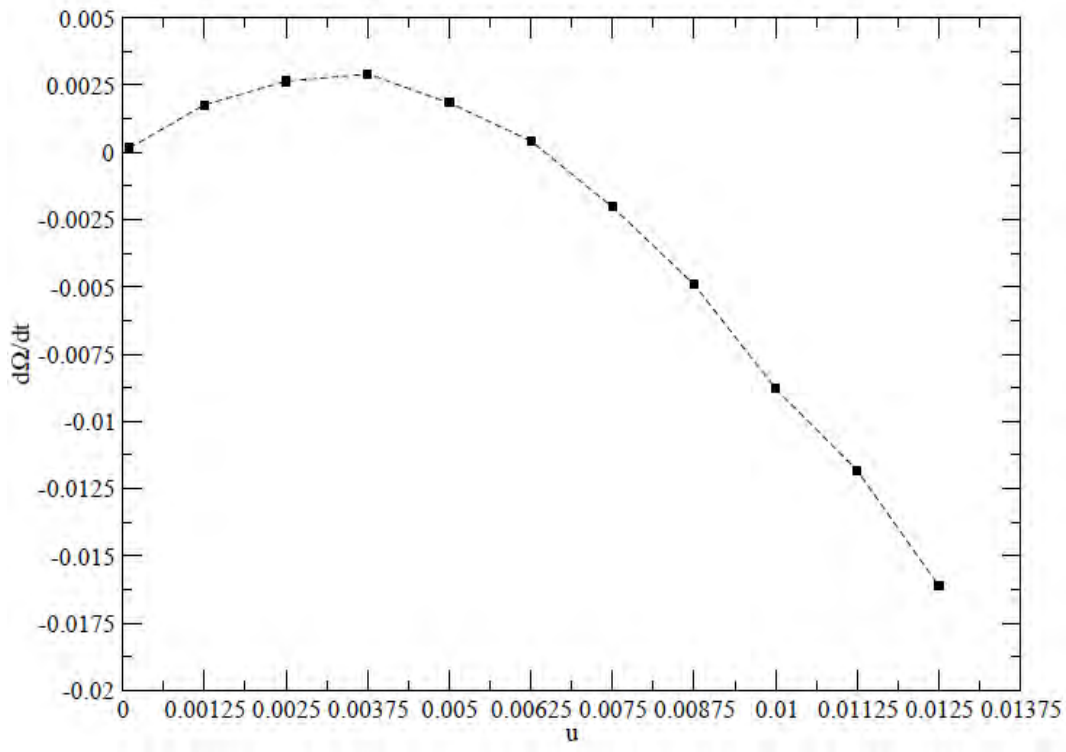

Figure 5.5: Objective function as a function of piston speed obtained in the range between Carnot efficiency and efficiency at maximum power. The function attains its maximum at 0.00375

In this second case of optimization, the objective function attains its maximum value when it takes piston speed of 0.00375. This piston speed is half of the piston speed obtained for the optimized efficiency when we consider the entire parameter value range, i.e the first case. The corresponding optimized efficiency is found to be 0.273 ± 0.002 and is equivalent to $0.91\eta_c$. As in the first case, this efficiency lies between the maximum efficiency and the efficiency at maximum power. The power that the engine delivers when working in this case is $0.522P_{max}$.

5.2 Discussions

Lets now make a more detail discussion about the results. First consider the temperature volume diagram as shown in Fig. 5.1. For u = 0.01, at the moment (initial points) when a heat reservoir is in contact with the system, the temperatures of the system are higher than T_h and lower that T_c and approaches the steady values soon. These results tell us during the adiabatic compression process, excess heat has been added to the system so that the system has attained a temperature higher than the temperature of the hot reservoir, T_h. Similarly, during the expansion process, the system has done much work and it is found to be at a lower temperature when the adiabatic expansion is completed. This phenomenon also happened for u = 0.001, but not much noticeable. When the engine enters into isothermal processes, it relaxes to attain a steady temperature.

We have discussed enough about the variation of the average power and efficiency with respect to piston speed. But we can say more about the optimized efficiencies for the two cases. In the first case we have seen that the optimized efficiency is 0.242 ± 0.002. This result is $0.81\eta_c$ where η_c is 0.3 for $T_h = 1.0$ and $T_c = 0.7$. This result agrees with those obtained in [14-16], who had made optimization studies on single level quantum dot [14], nano-scale photoelectric device at strong coupling [15]. In the second case, the optimized efficiency is 0.273 ± 0.002 and is equivalent to $0.917\eta_c$. This result is a good agreement to the analytical results obtained in [14]. In both cases we had obtained optimized efficiencies, but they are not equivalent in their importance. For example one may desire to use the optimized efficiency obtained in the first case but with lower efficiency compared to the optimized efficiency obtained in the second case. Even if the efficiency is lower, it is important to notice that the process is completed with time less than that of the second more efficient process. In fact according to the results, it takes a time of twofold to get an optimized efficiency higher than the one obtained when we

consider the entire parameter range (first case). Another benefit that can be obtained while working at the first optimized state is the amount of power that can be extracted from the engine. When the engine operates at this optimized state, the amount of power is higher than when it operates at the second optimized state by more than 30 percent.

Chapter 6

Summary and Conclusion

6.1 Summary

In this work, we have made a two-dimensional event-driven molecular dynamics simulation. We take the model as a cylinder with a piston moving back and forth at a constant speed u. The speed of the piston is taken to be a control parameter. The cylinder contains 100 hard discs (weakly interacting particles) which have each equal diameter of 0.01 and mass of 1.0. The system follows four steps to complete a single engine cycle. These are; adiabatic expansion in which the piston moves forward (expands) while the system is at constant temperature, which is ensured by connecting the cylinder with a heat reservoir at a temperature of T_h. After completing the isothermal expansion stage, the system enters to adiabatic expansion stage, where there is no transfer of heat energy into or out of the system. In this stage, the temperature of the system keeps decreasing as a result of loosing energy while doing work against the piston and finally attains a temperature of T_c. Now the cylinder is at its maximum volume and the next steps are compression processes. In the third step, the piston is compressed while it is in contact with a reservoir at temperature T_c. This is called isothermal compression. The fourth and final step involves disconnecting the reservoir and keeping compressing the piston until the cylinder attains

its initial volume (the volume of the cylinder before the first expansion step begins). Here the four processes all together form one complete cycle. We repeat the processes for a desired number of complete cycles depending on the speed of the piston. For example for larger piston speed values, the number of complete cycles are relatively larger than that of smaller piston speed values. In any case (for any physically acceptable piston speed values), we adjust the number of complete cycles in such a way that almost equal amount of time is taken by the piston.

We have calculated averaged quantities such as net work done and heat energy that flow in to the system from the reservoir at a temperature of T_h. From these two quantities, we have obtained the efficiency of the engine. We have seen that the efficiency approaches the Carnot efficiency for small piston speed values and vanishes when the piston speed is large. We take the control parameter (piston speed) range to be between the maximum efficiency (Carnot efficiency) and zero efficiency. When the piston speed is above a certain maximum value, the net work done becomes negative and we had rejected such piston speed values a they are nonphysical in the sense that they give negative efficiency. We had also calculated the average power as the net work done on the piston by the hard discs (gas molecules) divided by the total time elapsed. We obtained that the power attains a maximum value and vanishes when the piston speed is decreased or increased relative to the value of the piston speed where maximum power is attained.

The main result of this thesis is finding optimized efficiencies for the heat engine model considered. We make use of the unified optimization criterion developed by A. Calvo Hernandez et al [9] for any energy converter. They have developed an objective function that can be optimized and can let to obtain the optimum path that can make best compromise between useful effective energy and lost effective energy. In fact the objective function needs to fulfill three criteria according to the authors. One of the most

import criterion that the objective function should obey is not to depend on parameters that are not easily controllable. For the heat engine we considered, the piston speed is taken as a control parameter which is easily controllable. Since the objective function is explicitly dependent on the efficiency and power (which in turn depend of the control parameter), once we obtained the values of these quantities, it is easier to see the behavior of the objective function in terms of the piston speed. We exactly followed the above mentioned procedures and seen that the objective functions (for the two cases we considered) have exactly one maximum value for the physically allowed parameter value ranges. Once the value of the control parameter where the objective function attains its maximum value is identified, the (optimum) path that the engine need to follow so as to make the best compromise between lost useful energy and effective useful energy is known. We had obtained this optimum path for two kinds of (control) parameter value ranges. In the first case, we have considered the entire (physically acceptable) parameter value range. In this case we found that the optimized efficiency occurs when the piston speed is 0.0075. The (optimized) efficiency corresponding to this piston speed value is obtained to be 0.242 ± 0.002. In the second case we considered the range of the parameter to be between maximum efficiency and maximum power and obtained an optimized efficiency of 0.273 ± 0.002. We have seen that both optimized efficiencies lie between the maximum efficiency and the efficiency at maximum power.

In table 6.1, we summarize the results by comparing the optimized efficiencies with the Carnot efficiency, the optimized powers with the maximum power and the time taken at optimized states with the time taken at maximum power.

Table 6.1: Comparison of optimized efficiencies, power and time with respect to Carnot efficiency, maximum power and time taken at maximum power.

Physical Quantity	**Relative Value**
η_{mp}	$0.67\eta_c$
η_{opt1}	$0.81\eta_c$
η_{opt2}	$0.91\eta_c$
P_{opt1}	$0.84P_{max}$
P_{opt2}	$0.52P_{max}$
t_{opt1}	$1.67t_{mp}$
t_{opt2}	$3.33t_{mp}$

6.2 Conclusion

From the results of event-driven molecular dynamics simulation, we have seen that the behavior of the heat engine model we considered approaches the properties of the quasi-static Carnot cycle. For example, the plot of temperature versus volume shows that for small piston speed values, the deviation of the finite time cycle is smaller compared to the quasi-static process. We have also seen that the Carnot efficiency is approached for small piston speed values. We have seen that the average power of the heat engine exhibits a maximum value. The most important result we found is the optimized efficiency. We have seen in chapter 3, it is possible to have an optimized efficiency that lies between the maximum efficiency and the efficiency at maximum power. We find the optimized efficiencies by taking the unified optimization criterion [9] for heat engines. In fact from our work as well as the results obtained in [14-16] show that the optimized efficiency is independent of the nature of the heat engine model considered and shows some sort of universality.

Bibliography

[1] Dilip Kondepudi and Ilya Prigogine, Modern Thermodynamics, from heat engines to dissipative structures (John Wiley and Sons, 1998).

[2] H. T Odum and R. C Pikerton Am. Sc. **43**, 331 (1955).

[3] F. L. Curzon and B. Alhborn, Am. J. Phys. **43**, 22 (1975).

[4] M. Esposito and K. Lindenberg, PRL 102, 130602(2009).

[5] M. Esposito, R. Kawai, K. Lindenberg, C. Van den Broeck, arXiv: 1008. 2464v2[Cond-mat. stat-mech]1 Sept. 2010.

[6] T. Schmiedl and U. Seifert, EPL, 81(2008) 20003.

[7] M. Esposito, K. Lindenberg and C. Van den Broeck, EPL, 85(2009)60010.

[8] Z C Tu, J. Phys. A:math. Theor. 41(2008)312003(6pp).

[9] A. Calvo Hernandez, A. Medina, J. M. M. Roco, J. A. White, and S. Velasco, Phys. Rev. E, **63**, 037102 (2001).

[10] Y. Izumida and K. Okuda, EPL, **83** (2008) 60003.

[11] Morten Hjorth-Jensen, Computational Physics (University of Oslo, Fall 2006).

[12] J. M. Haile, Molecular Dynamics Simulation, Elementary Methods (John Wiley and Sons, 1992).

[13] M. P. Allen and D. J. Tildesley, Computer Simulation of Liquids (Clarendon Press. Oxford, 1991).

[14] Fitsum Borga and Mulugeta Bekele, Msc thesis, Addis Ababa University, Addis Ababa 2010 (unpublished).

[15] Simachew Endale and Mulugeta Bekele, Msc thesis, Addis Ababa University, Addis Ababa 2010 (unpublished).

[16] Solomon Worku and Mulugeta Bekele, Msc thesis, Addis Ababa University, Addis

Ababa 2010 (unpublished).
[17] Y. Izumida and K. Okuda, arXiv: 0907. 4868v1[Cond-mat. stat-mech] 28 July 2009.

Declaration

This thesis is my original work, has not been presented for a degree in any other University and that all the sources of material used for the thesis have been dully acknowledged.
Name: Mehari Bayou

Signature:

Place and time of submission: Addis Ababa University, December 2010

This thesis has been submitted for examination with my approval as University advisor.
Name: Dr.MULUGETA BEKELE

Signature: